(4)

UNLIMITED
UNCLASSIFIED

Canada

THE ORBITAL-PLATFORM CONCEPT FOR NONPLANAR DYNAMIC TESTING

by
M.E. Beyers and X.Z. Huang
National Aeronautical Establishment

OTTAWA
MAY 1988

AERONAUTICAL NOTE
NAE-AN-52
NRC NO. 29133

National Research Council Canada
Conseil national de recherches Canada

UNLIMITED
UNCLASSIFIED

THE ORBITAL-PLATFORM CONCEPT FOR NONPLANAR DYNAMIC TESTING

LE CONCEPTE DE LA PLATE-FORME ORBITALE POUR LES ESSAIS DYNAMIQUES NON-PLAN

by/par

M.E. Beyers and X.Z. Huang

National Aeronautical Establishment

AERONAUTICAL NOTE
NAE-AN-52
NRC NO. 29133

OTTAWA
MAY 1988

K.J. Orlik-Rückemann, Head/Chef
Unsteady Aerodynamics Laboratory/
Laboratoire d'aerodynamique instationnaire

G.F. Marsters
Director/Directeur

ABSTRACT

A new concept is introduced for large-amplitude nonplanar testing at high incidence. The dynamic test apparatus is characterized by an annular, orbital platform on which the model support and secondary drive mechanisms are mounted. The device can be used as a rotary apparatus, while arbitrary epicyclic motions (including fixed-plane, orbital modes) and oscillatory motions superimposed on the coning mode may be generated. The system is inherently very rigid and vibration levels can be kept very low. Aerodynamic interference is also very low as there is no need for bulky support hardware and the test section is circular. Accordingly, the system may be used to assess levels of support interference in conventional rotary tests.

RÉSUMÉ

Cette étude traite d'un nouveau concept dans le domaine du testing à forte amplitude suivant des degrés de liberté multiples et à grande incidence. L'appareil de testing dynamique se caractérise par une plate-forme annulaire qui gravite en orbite. Le support de la maquette et le mécanisme d'entraînement secondaire sont montés sur la plate-forme. Toute l'instrumentation peut-être utilisée comme une balance rotative, pendant que les mouvements épicycloïdaux et oscillatoires superposés en mode de conicité peuvent être induits. Tout le système est fort rigide, ce qui permet de garder un niveau très bas de vibration. L'interférence aérodynamique est également minime étant donné qu'on a pas besoin de superstructure massive de support et parce que la section de testing est circulaire. En conséquence, le système peut-être utilisé pour évaluer les niveaux d'interférence dans le testing conventionnel faisant appel à des systèmes rotatifs.

CONTENTS

LIST OF ILLUSTRATIONS

NOMENCLATURE

A	= transformation matrix
b	= wingspan
I_{yz}	= cross product of inertia
K_1, K_2, K_3	= tricyclic vectors
p, q, r	= body-axes angular velocities
r_0	= orbital radius or spin radius
u, v, w	= body axes velocity components
V_∞	= freestream velocity
w	= test section width
x, y, z	= body axes system
X, Y, Z	= inertial frame of reference
α	= angle of attack = $\tan^{-1}(w/u)$
β	= angle of sideslip = $\sin^{-1}(v/V_\infty)$
Γ	= balance angle of pitch
Λ	= tangential tilt angle
ν_2	= secondary oscillation frequency
ξ, υ, ζ	= platform frame of reference
σ	= total angle of attack
ϕ_o	= model roll angle
$\dot{\phi}_1, \dot{\phi}_2$	= epicyclic vector rates
Φ	= orbital roll angle
ψ, θ, ϕ	= Euler angles
ψ_m, θ_m, ϕ_m	= modified Euler angles
Ψ	= sting-shaft roll angle
ω	= orbital or coning angular velocity
$\bar{\omega}$	= reduced circular frequency = $\omega b/(2V_\infty)$
Ω	= reduced orbital frequency = $\omega r_0/V_\infty$

Superscripts

$(\bar{\ })$	= fixed-plane system
$(\tilde{\ })$	= nonrolling angles
$(\dot{\ })$	= differentiation with respect to time

Abbreviations

DOF	degree of freedom
LSWT	NAE 2 m × 3 m Low Speed Wind Tunnel
OPLEC	orbital-platform epicyclic coning

1. INTRODUCTION

The importance of motion shape and history in vehicle dynamics is being increasingly recognized[1-4]. The nature of the coupling between vehicle motion and flow separation has been analyzed for precessing missiles[5] and aircraft in limit-cycle[6] or spinning motions[7] at high α. Following this thrust, the need for experimental[8,9] and numerical[10] studies of nonplanar motion aerodynamics has been pointed out. While CFD techniques are still limited, for instance, by the need for turbulence modelling, these methods may ultimately provide the means for studying time-history effects in the general case; motion history can probably be reproduced experimentally only in special cases. On the other hand, the possibilities for simulation of fairly general periodic nonplanar motion types in the laboratory appear quite promising[9].

Rotary balances have traditionally provided the aerodynamic data used as a basis for stall-spin investigations[11]. Since angular rates representative of full-scale aircraft spinning behaviour can be achieved in a simple coning experiment[12], a good experimental simulation of the helical mode is possible. However, rotary balance testing in its present form is not without experimental difficulties, the most serious of which are probably support interference[13] and in some cases, unsteady wall interference[14] and vibration.

The well-known nonplanar aircraft mathematical model, due to Tobak an Schiff[4], specifies characteristic motions comprising small amplitude oscillations superimposed on high-rate coning motions. The need for an experiment involving these characteristic motions has been pointed out[4,15,16] but this goal has yet to be realized. However, an experimental technique based on the orbital motion principle[17] has been proposed for the simulation of the oscillatory spin of a fighter aircraft[9].

In this Note a unique rotary testing concept is proposed that offers possibilities for reduction of aerodynamic interference and for extension to 2-degree-of-freedom (DOF) experiments. This design is a further development of the horizontal-axis configuration of the conceptual orbital motion apparatus[8,17]. Its implementation in a workable mechanical system draws from bearing concepts considered for application to rotating balances[18].

2. DEVELOPMENT OF THE CONCEPT

As noted above, the impetus for the development of a new rotary testing concept was provided by considerations of aerodynamic interference in tests on existing apparatuses and from the need for extension to high-α nonplanar motions. The rationale for 2-DOF experiments was alluded to in the Introduction and will be further discussed in Section 4. Before proceeding with the development of the test technique it will be instructive to review the nature of the interference problem in rotary balance tests.

2.1 Aerodynamic Interference

Support interference arises largely as a consequence of the rotating strut and counterweight or other pitch adjustment mechanisms, which, of necessity, become bulky when deflections are to be kept to acceptable levels in high-speed and/or pressurized facilities (See Fig. 1). (Since the rotating strut is often curved, it is referred to as such.) The distortion of the vortex systems shed from the aircraft forebody and lift surfaces at high α could be significant except within the coning-induced sideslip angle range such that the vortex wake passes clear of the curved strut. Interference may be present even in this β range since the vortex trails will intersect the sheet of vorticity shed behind the rotating strut. Since the sting itself can contribute appreciable interference in the top-entry configuration, there is not much to be gained in using this method of setting high pitch angles in favour of reducing the span of the curved strut. A detailed discussion of support interference effects in coning tests of forebody-dominated shapes is given in Ref. 13.

When unsteady wall interference is present, the steady nature of the rotary flow breaks down. While this is not a concern in most rotary tests, there are instances, particularly in high-speed, pressurized tunnels, where wall effects could be large. The principal mechanisms of unsteady interference are transverse acoustic interference and vortex-wake/wall interference. Transverse acoustic interference[14] (see Fig. 2) can result in a resonance-like phenomenon in large low-speed facilities. In contrast, vortex/wall interference can occur in facilities of any size and depends on the reduced rate, $\omega b/(2V_\infty)$, and effective span-to-width ratio, b_s/w. Since the rotating strut usually has the largest transverse dimension the phenomenon is normally produced by the strut tip vortices, which can cause separation on the walls to fluctuate as illustrated in Fig. 1. While no unsteady interference data are available from rotary tests, some relevant results from forced oscillation-in-yaw experiments are available, demonstrating that the interference can become large under special circumstances.

When wall interference is present it will be superimposed on the effects of support interference. The overall effects on the aerodynamic measurements are due to deflection of the vortex system in a quasi-steady sense and to time lag effects. In conventional rotary balance tests the latter may not be a concern since only the integrated DC outputs are recorded. On the other hand, in any unsteady experiments, or even in tests requiring more refined steady measurements, aerodynamic interference could become a limiting factor since the effects of support and wall interference are not easily separated[14].

With these thoughts in mind, it becomes tempting to consider an alternative arrangement by means of which complete sources of interference can be eliminated: If the walls could be replaced by a perfectly circular section and if the rotating strut could be eliminated, then both wall and support interference would disappear for practical purposes. This is exactly the objective pursued in the next Section.

2.2 The Annular Orbital Platform

One clue to the way in which the rotary experiment can be restructured is offered by the orbital motion scheme depicted in Fig. 3. This is a simplification of the general arrangement[17] obtained when the orbital axis is horizontal (i.e. not inclined). There are two axes providing continuous rotations Φ and Ψ, which may be mutually inclined through a tilt angle Λ. The sting and balance are supported on the orbital platform, which is of arbitrary shape. If this shape is taken to be a cylindrical surface aligned with the axis, the results obtained are interesting for now the sting may be directed inwards with the model located on the axis of rotation at a nonzero pitch angle. An arrangement is obtained where the annular platform could be flush with the walls in a circular test section, or outside the flow as in a vertical open-jet tunnel, as illustrated in Fig. 4. Since most of the support hardware is outside the circular test section, the aerodynamic interference should be very low. Such an annular configuration was considered in the context of gas-bearing applications to rotary balances[18].

The Nomenclature defined in Fig. 3 is used for the description of the fixed-plane orbital modes[17]. In analyzing general 2-DOF motion it is more convenient to use Euler angles to define the orientation of the model, with the coning axis aligned with the wind as shown in Fig. 5. (For arbitrary motion shapes two additional variables are needed.)

The orbital platform concept as adapted to a vertical spin tunnel (Fig. 4) was originally considered as a possible installation in the NAE 4.6 m Vertical Wind Tunnel, but the idea was dropped since its usefulness would have been limited by the tunnel performance. Moreover, since circular test sections are something of a rarity, it was considered more desirable to adapt the concept to test sections of arbitrary shape and, in particular, to the modified rectangular section of the NAE 2 m × 3 m Low Speed Wind Tunnel (LSWT).

This requirement of universality resulted in the notion of a cylindrical installation, housing the annular platform assembly, that would be mounted inside the working section. Since the concept is characterized by an orbital platform with a mechanism providing a secondary DOF, it is referred to here as the OPLEC concept, for "orbital-platform epicyclic coning" system.

2.3 Mechanical Design

The OPLEC concept can now be developed into a workable design. Mechanical details are included as required to provide the various dynamic testing features alluded to above. The resulting mechanical layout is illustrated schematically in Fig. 6 and 7.

As shown in Fig. 6, the test facility comprises a cylindrical test-section insert of circular cross-section, mounted on a vertical support strut between the floor and roof of the LSWT. The tubular section is further anchored by means of a number of tension cables attached to the rectangular walls. The main drive system consists of a

stepping motor mounted on the roof of the LSWT working section and a drive shaft within the strut. The drive pinion engages a webless bevel gear attached to the downstream end of the annular platform as shown in Fig. 7. The aft portion of this rotating section is covered by a stationary tubular section which makes up the aft circular test- section wall. The exposed portion of the rotating cylinder is denoted the "orbital platform", upon which the model support and secondary drive mechanism are mounted. The leading edge and forward test-section wall of the device is a stationary splitter-plate/fairing designed to provide parallel flow within the test section. The rotating cylinder runs on a set of three ball bearings mounted in an outer cylindrical casing which is integral with the main strut. An annular housing is provided for mounting a counterweight and dynamic balance masses.

The model is sting-mounted with its reference centre on the rotation axis and a flange at the end of the sting/drive-motor assembly is bolted directly to the orbital platform. Additional lateral location is provided by two lateral telescopic struts attached to stub shafts that are integral with the sting. A high degree of structural rigidity is afforded by this three-point attachment method. An angle-of-attack change is accomplished as shown in Fig. 8. The sting support strut is replaced by one of a set of struts, each corresponding to a particular pitch angle and a fixed reference centre, while the lateral telescopic struts are extended and clamped at the appropriate attitudes and lengths required to complete the triangulation.

A simple circular sting with mounting flange may be used in coning or steady spin tests at nonzero spin radius (see Fig. 9). More complex, 2-DOF motions may be generated by means of a secondary-drive, stepping motor located within a housing integral with the sting as shown in Figs. 7 and 8 and connected to the balance by a countershaft free to rotate within the sting. Thus, epicyclic motions are obtained by rotating the model around the sting axis, while alternatively, a conventional, inexorable pitch-oscillation mechanism driven by the same stepping motor could be used to generate pitching or yawing oscillations superimposed on the steady coning motion.

The loads on the model are sensed by a 5-component dynamic balance. The balance signals are transmitted by FM telemetry over the gap between the rotating platform and the casing and the signals are fed via a conduit in the strut to the front-end of the data-aquisition system. When the secondary drive is used, an external pulse source is required. The control unit is located outside the LSWT working section and the pulsed power is transmitted via a series of rolling carbon-tipped disc conductors in an insulated assembly (Fig. 7). For the case where the model rotates relative to the sting, a second FM telemetry link is provided to transmit the signals between the balance and the forward part of the hollow sting. A commercially-available FM unit may be used here, following the practice in Magnus balance design.

2.3.1 Design options

The design described is based on ideas which are straightforward to implement in the interest of saving time, more exotic features may be appropriate if expediency is not the main consideration

For instance, the use of gas bearings rather than ball bearings would introduce several advantages[18]. Whereas conventional bearings are limited by surface speed of the balls or rollers, to a rotation rate of perhaps 15 Hz, depending on the dynamic loads, very high rotation rates can be achieved on air bearings. On the other hand, most full-scale steady spins are in the range $\bar{\omega} \leq 0.2$,[12] which corresponds to a limit of about 12 Hz on the present scale; thus, the performance of ball bearings would probably be adequate. A second advantage of gas bearings lies in the possibility of lower noise levels, since vibration levels are likely to be reduced by the damping effect of the air cushion.

2.4 External Orbital-Platform Configuration

An important variation of the design concept is arrived at when the orbital platform and annular support housing are inverted. Then the interior becomes a stationary circular duct and the orbital platform rides on its external surface, again using air or ball bearings. This is similar to the original concept for a vertical tunnel (Fig. 4). As will be shown below, although less versatile, this concept could be aerodynamically superior at high α, while the internal orbital platform (Fig. 7) is more suitable if the complete α range has to be covered.

As illustrated in Fig. 10, the external configuration requires externally-mounted struts, while the model is mounted forward of the leading edge of the splitter-fairing. Flow disturbances inside the duct are effectively eliminated if the orbital platform is located a short distance downstream of the leading edge and the struts are swept forward as shown. A larger model scale may be used in this layout, for a given test section size, but the advantage may be partly offset by the larger cross-sectional area of the struts and disc conductor assembly. In other words, the model is larger in relation to the orbital platform but the latter might have to be reduced in diameter to keep the blockage area within acceptable limits. Of course, if the wind tunnel has a circular working section, then the full diameter is available and the blockage is negligible as in the vertical wind tunnel. The largest suitable ball races available commercially are perhaps 1.5 m in diameter, hence, gas bearings[18] have to be used for large-scale testing applications. This is quite feasible provided that the large-diameter external circular surfaces can be ground. In this respect, the vertical tunnel concept (Fig. 4) has the advantage, since grinding will be required only for flat surfaces providing vertical location; the external circular surfaces for lateral location may be machined.

There is some increase in mechanical complexity associated with the bent lateral telescopic struts and some loss in rigidity. However, the main drawback of the external orbital platform is that it becomes impracticable at pitch angles below about 30° when a secondary drive motor is to be used (Fig. 10). From the aerodynamic point of view, this system has the advantage of no moving surfaces within the duct, while the flow disturbances associated with the presence of the secondary drive mechanism are diverted into the region between the annulus and the wind tunnel walls, where it cannot produce any aerodynamic interference on the model. On the other hand, the model is

located in the open rectangular working section with its wake partly enclosed in the circular duct, resulting in more complex aerodynamic design considerations (see Section 3.2).

3. ANALYSIS OF THE DESIGN

The salient characteristics of the OPLEC concept are the orbital platform and the circular cross-section of its test section. An analysis of these features point to certain natural advantages over the conventional rotary balance configuration. There may also be some disadvantages, such as the need for one or two FM links to transmit the balance signals, but for the most part, these are not expected to be restrictive in the sense of, for instance, the effects of support interference in conventional rotary balance tests.

3.1 Rigidity

Perhaps the most obvious advantage of the OPLEC device is the high rigidity of the model support. For the purposes of the discussion, the two fundamentally different rotary balance configurations are approximated structurally by the elements shown in Fig. 11. The conventional system may be thought of as a cantilever beam and the OPLEC support as a truss with a short cantilever extension. A greatly simplified analysis shows the linear deflections to be proportional to L^3 and the stiffness inversely proportional to L^3, where L is the effective beam length. For the conventional rotary apparatus L is roughly equal to the sum of the lengths, $\ell_1+\ell_2+\ell_3$. Then, from Fig. 11 it follows that the effective length of the OPLEC cantilever is no more than 1/3 of its counterpart in the conventional system. Thus, the model support will be an order of magnitude stiffer in the former case. The external orbital platform configuration will be somewhat less stiff, but, nevertheless, far more rigid than the conventional system.

3.2 Aerodynamic Interference

As suggested in Section 2.1, the OPLEC concept results in greatly reduced aerodynamic interference. The support interference caused by the interaction of vortices shed from the aircraft model with the curved strut and its vortex wake, as illustrated in Fig. 1, is absent in the OPLEC configuration. As will be appreciated from Figs. 6 and 7, the separated model wake is completely separate from that shed behind the sting and lateral struts at high α, while even at low incidence the cross-section of the support structure is smaller than in the conventional setup. Moreover, unlike the latter case, flow separation on the walls caused by interaction of the vortex wake with the wall boundary layer will be steady in relation to the rotating model by virtue of the circular test section (Fig. 1). This effect is even further reduced in the external orbital-platform configuration, when the disturbance along the wall is a minimum because of the small cross-section of the strut system. By extension, the direct interaction of the vortex-wake with the circular wall results in a constant deflection of the wake trail as illustrated in Fig. 12. Both sources of wall interference, therefore, reduce to a fixed angle-of-attack change at the walls which may be corrected for following the procedure used in propeller tests[19].

In the internal orbital-platform apparatus a possible source of interference is the flow rotation caused by the rotating platform and sting. This moving-wall effect is not expected to be significant. Note that the width of the orbital platform can be reduced by the use of a stationary cover over the aft portion, depending on the placement of the struts. The sting and struts are, of course, a source of interference in themselves, sinces their wakes will cause separation on the walls. Again, this disturbance is expected to be relatively small. A more serious type of interference is produced by a top-mounting installation, as might be required in certain epicyclic modes (see Section 4.1.2).

The internal orbital-platform apparatus is well-suited to the investigation of support interference in conventional rotary balance tests. Since there are both rotating and stationary sections of the circular test section, replicas of the curved strut and the support strut can be respectively mounted on the orbital platform and on the aft circular section as shown in Fig. 13, to simulate the effect of the support in a rotary balance test. The incremental aerodynamic loads due to the presence of the curved strut can then be determined directly. Since the test section is circular no unsteady wall interference will be present, and given the low base interference of the OPLEC strut system, the interference due to the dummy struts will be approximately equivalent to the difference between the loads measured with and without the dummy struts.

3.3 Vibration

Vibration of the support and tunnel walls can present a problem in rotary tests involving unsteady measurements. Mass unbalance is, perhaps, the major source of vibration. Unlike the conventional rotary balance configuration, which cannot be dynamically balanced, the OPLEC system provides for dynamic balance masses to be mounted in an annular enclosure adjacent to the orbital platform (see Fig. 7). As illustrated schematically in Fig. 14, the correct placement of a static counterweight and three dynamic balance masses would eliminate the cross products of inertia

$$\sum I_{yz} = 0 \qquad (1)$$

while, from symmetry considerations, the other products of inertia would also be zero.

In principle, a perfect dynamic balance can be achieved with the internal orbital-platform apparatus. This will be more difficult for the external configuration since, in this case, it is desirable to keep the orbital platform short; nevertheless, the dynamic balance could be quite good, particularly for the high-α installations.

4. CHARACTERISTIC MOTIONS

A detailed discussion of the characteristic motions which can be generated by means of the OPLEC system is beyond the scope of this Note. Many of the kinematical relationships have been presented elsewhere[9,17]. However, the basic relationships peculiar to the OPLEC geometry are derived here. The characteristic motions fall into two general categories, epicyclic and oscillatory motions.

4.1 Epicyclic Motion

When the two rotations in Fig. 5 are independent, $|\dot{\phi}| \neq |\dot{\psi}|$, the resulting motions comprise two superimposed components which may have different frequencies and amplitudes. Such motions are epicyclic and may, therefore, be described by two fixed-amplitude vectors rotating in the $i\tilde{\alpha}$, $\tilde{\beta}$ plane as shown in Fig. 15[9]

$$\tilde{\beta} + i\tilde{\alpha} = K_1 e^{i\dot{\phi}_1 t} + K_2 e^{i\dot{\phi}_2 t} \tag{2}$$

K_1 and K_2 are the complex vector amplitudes and $\dot{\phi}_1$, $\dot{\phi}_2$ the angular rates. The angles $\tilde{\beta}$, $\tilde{\alpha}$ describe the orientation of the aircraft longitudinal axis in the nonrolling frame of reference. At high angles of attack it would be more correct to represent the motion by a projection on a spherical surface rather than on a plane but the basic principle is the same.

4.1.1 1-DOF motion

When $K_1 = 0$, lunar coning is obtained (see Fig. 16(a)); this is, of course, the most basic 1-DOF nonplanar motion. In the present nomenclature, the rotation about the velocity vector is given by the rotation rate $\dot{\psi}$ and pitch angle θ (Fig. 5). Continuous rolling or spinning at nonzero α can be obtained from a rotation $\dot{\phi}$ about the x axis with $\dot{\psi} = 0$ and $\theta \neq 0$.

4.1.2 2-DOF motion

In the general case, assuming $\dot{\psi}_m$ is small, Eq. 2 yields the aerodynamic angles expressed in the fixed-plane system

$$\begin{aligned} \bar{\alpha} &= A_1 \cos\dot{\phi}_1 t + B_1 \sin\dot{\phi}_1 t + A_2 \cos\dot{\phi}_2 t + B_2 \sin\dot{\phi}_2 t \\ \bar{\beta} &= B_1 \cos\dot{\phi}_1 t - A_1 \sin\dot{\phi}_1 t + B_2 \cos\dot{\phi}_2 t - A_2 \sin\dot{\phi}_2 t \end{aligned} \tag{3}$$

The precessional and the nutational vectors K_1 and K_2 describe a true epicyclic motion as illustrated in Fig. 16(b). Note that when the secondary rotation is along the model longitudinal axis the motion described by the model nose is circular, but the angle-of-attack variation is still epicyclic. When the model longitudinal axis is inclined with respect to the ψ axis as in Fig. 3, $\Gamma \neq 0$, or inclined out of the plane of θ with $\Lambda \neq 0$ and $\theta \neq 0$ (Fig. 5), a more general motion is obtained. This may be thought of as a pitching and yawing oscillation superimposed on the steady coning motion. However, it should be noted that this motion is not exactly the same as that obtained with the orbital geometry depicted in Fig. 3 since the epicyclic vector rates are reversed in this case. Moreover, the case $\Gamma \neq 0$ requires top-mounting unless Γ is limited to small angles.

The reference systems are depicted in Fig. 17. The transformation between the inertial and body axis is given by (for $\Gamma = 0$)

$$\begin{bmatrix} y \\ z \\ x \end{bmatrix} = [A] \begin{bmatrix} Y \\ Z \\ X \end{bmatrix} \tag{4}$$

where

$$[A] = \begin{bmatrix} \cos\phi\cos\psi-\sin\phi\cos\theta\sin\psi & \cos\phi\sin\psi+\sin\phi\cos\theta\cos\psi & \sin\phi\sin\theta \\ -\sin\phi\cos\psi-\cos\phi\cos\theta\sin\psi & -\sin\phi\sin\psi+\cos\phi\cos\theta\cos\psi & \cos\phi\sin\theta \\ \sin\theta\sin\psi & -\sin\theta\cos\psi & \cos\theta \end{bmatrix} \tag{5}$$

Then the body axes velocity components are, for nonzero orbital radius[17],

$$\begin{bmatrix} v \\ w \\ u \end{bmatrix} = [A] \begin{bmatrix} -\dot{\psi} r_0 \sin\phi \\ \dot{\psi} r_0 \cos\phi \\ V_\infty \end{bmatrix} \tag{6}$$

The aerodynamic angles α and β are then directly related to the Euler angles through the definition

$$\begin{aligned} \alpha &= \tan^{-1}(w/u) \\ \beta &= \sin^{-1}(v/V_\infty) \end{aligned} \tag{7}$$

The transformation of the angular velocities is given by

$$\begin{bmatrix} q \\ r \\ p \end{bmatrix} = \begin{bmatrix} \sin\theta\sin\phi & 0 & \cos\phi \\ \sin\theta\cos\phi & 0 & -\sin\phi \\ \cos\theta & 1 & 0 \end{bmatrix} \begin{bmatrix} \dot{\psi} \\ \dot{\phi} \\ \theta \end{bmatrix} \tag{8}$$

Eq. (8) shows that, in general, all three body-axes angular rate components are nonzero. A suitable choice of the motion parameters could yield a motion representative of an oscillatory spin. However, it is possible that the geometry of Fig. 3 would provide the closest analogue of this flight mode. Note that the captive epicyclic modes are all pure and not subject to any frequency or amplitude restrictions. The only factor to detract from the fidelity of the motions would be small distortions due to deflections of the support system under inertial and aerodynamic loads, which are eliminated for practical purposes in the OPLEC concept.

4.2 Nonplanar Oscillatory Motions

Two families of nonplanar oscillatory motions can be generated; namely, the degenerate modes of epicyclic motion (fixed-plane orbital motions[17]) and composite motions obtained by superimposing planar oscillatory motions on the coning mode. The fixed-plane motions are characterized by two coupled DOFs (one independent DOF).

4.2.1 Fixed-plane orbital motion

The fixed-plane modes have been analyzed in considerable detail[17] and it will suffice to show here that some of the kinematical relationships for the horizontal orbital axis can be derived from Eqs. (4) to (8). The associated characteristic motions are pure translation ($p = q = r = 0$) and fixed-plane coning at arbitrary incidence. For the pure rotational mode it is necessary to revert to the orbital motion geometry of Fig. 3. The fixed-plane constraint is

$$\phi = -\psi \tag{9}$$

In the translational mode (Fig. 18(a)) the model is tilted at an angle Γ relative to the sting axis and $\theta = 0$ (Fig. 5). Then, performing a rotation through ψ and ϕ, given by Eq. (6), followed by a rotation through Γ, Eq. (7) yields

$$\begin{aligned} \beta &= \sin^{-1}\{-\Omega\sin\psi\} \\ \alpha &= \tan^{-1}\{(\tan\Gamma + \Omega\cos\psi)/(1-\Omega\cos\psi\tan\Gamma)\} \end{aligned} \tag{10}$$

$$\begin{aligned} \dot{\beta} &= -\omega\Omega\cos\psi \\ \dot{\alpha} &= -\omega\Omega\sin\psi \end{aligned} \tag{11}$$

where $\Omega = \omega r_0/V_\infty$ and terms in Ω are neglected. The fixed-plane coning mode is obtained directly from Eq. (7) and (9) ($r_0 = 0$).

In the pure rotational mode (Fig. 18(b)), $\theta = 0$ and $\Gamma \neq 0$ and the sting axis is tilted at the helix angle $\Lambda = -\Omega$, as in Fig. 3. Then it may be shown that

$$\alpha = \Gamma;\ \beta = \dot{\beta} = \dot{\alpha} = 0 \tag{12}$$

and

$$\begin{aligned} p &= \omega\Omega\cos\psi\sin\Gamma \\ q &= \omega\Omega\sin\psi \\ r &= -\omega\Omega\cos\psi\cos\Gamma \end{aligned} \tag{13}$$

4.2.2 2-DOF composite motions

Characteristic motions specified in the Tobak-Schiff[4] mathematical model applicable when the dependence on coning rate is nonlinear and the swerving is small are depicted in Fig. 19 and 20, respectively, for the aerodynamic and body axes systems. These characteristic motions can be generated exactly by means of the dual drive mechanism of the OPLEC system.

Since the OPLEC method is quite general any secondary DOF waveform may be generated; however, harmonic perturbations are considered in the context of this mathematical model. Then the angular velocity in the pitch-oscillation-coning mode (Fig. 19), as obtained from Eq. (8), is

$$\begin{bmatrix} q \\ r \\ p \end{bmatrix} \begin{bmatrix} \sin\theta\sin\phi & 0 & \cos\phi \\ \sin\theta\cos\phi & 0 & -\sin\phi \\ \cos\theta & 1 & 0 \end{bmatrix} \begin{bmatrix} \dot{\psi} \\ 0 \\ \dot{\theta}_0 \sin\nu_2 t \end{bmatrix} \tag{14}$$

and, in roll-oscillation coning,

$$\begin{bmatrix} q \\ r \\ p \end{bmatrix} = \begin{bmatrix} \sin\theta\sin\phi & 0 & \cos\phi \\ \sin\theta\cos\phi & 0 & -\sin\phi \\ \cos\theta & 1 & 0 \end{bmatrix} \begin{bmatrix} \dot{\psi} \\ \dot{\phi}_0 \sin\nu_2 t \\ 0 \end{bmatrix} \tag{15}$$

where ν_2 is the secondary frequency of oscillation. The angular velocity in the yaw-oscillation-coning mode (Fig. 20) is obtained in a similar fashion from Eq. (8) but this transformation is then followed by a rotation through the angle $\Delta\psi_m \cos\theta_m$ measured about the body yaw axis.[17] The derivation of this expression is omitted here for the sake of brevity.

The rate of change of α and β due to the rotational motion are given by

$$\begin{aligned} \dot{\alpha} &= q - (p\cos\alpha + r\sin\alpha)\tan\beta \\ \dot{\beta} &= p\sin\alpha - r\cos\alpha \end{aligned} \tag{16}$$

The combination of the basic coning mode with the two oscillatory modes given by Eqs. (14) and (15) represent a complete set of characteristic motions in the aerodynamic axes system (Fig. 19) and similarly for the body axes system (Fig. 20). When $\dot{\psi} = 0$, the conventional, planar oscillatory motions are, of course, obtained.

5. CONCLUSIONS

A new aerodynamic testing concept was introduced in this Note as a response to the need for increased versatility in dynamic testing and for reducing aerodynamic interference in such tests. The OPLEC method is characterized by an orbital platform used to mount the model support and secondary drive mechanisms. For application to non-circular working sections a circular sub-test-section is used to house the rotating hardware. Both internal and external orbital-platform configurations were considered. Based on the analysis of these concepts, the following conclusions may be drawn.

a. The OPLEC system can be used to generate a wide range of characteristic motions required in mathematical models of aircraft dynamics, including coning, arbitrary epicyclic motions, and oscillatory motions superimposed on the coning mode.

b. The modes of fixed-plane orbital motion associated with a non-inclined axis may also be obtained, including pure translation, pure rotation and fixed-plane coning at arbitrary incidences.

c. The OPLEC system is inherently most rigid and vibration levels can be kept very low by virture of the capability for dynamic balancing.

d. Aerodynamic support interference is very low in both OPLEC configurations as the need for bulky rotating hardware is eliminated.

e. Unsteady wall interference is, for practical purposes, absent in the internal-platform configuration and could be negligible in the external arrangement. However, a steady flow deflection may be present, which can be corrected for.

f. The levels of support interference in conventional rotary balance tests may be assessed in experiments involving representative "dummy" installations in the OPLEC test section.

g. The internal-orbital platform configuration of OPLEC facilitates nonplanar testing at arbitrary angles of attack, while the external arrangement is most suitable at high α. High rotation rates are feasible with both configurations.

h. The external-platform configuration is suitable for large-scale aerodynamic testing and can readily be adapted to a vertical spin tunnel. In contrast, the internal-platform arrangement offers somewhat greater versatility, and is, therefore, more attractive as a scientific tool.

6. ACKNOWLEDGEMENT

The authors gratefully acknowledge the contributions of Mrs. H. Cuccaro, Mrs. J. Fyffe, Stenographic Services (typing), Mrs. N.L. Daly and Mrs. M. Bédard (report production).

7. REFERENCES

1. Murphy, C.H., "An Erroneous Concept Concerning Nonlinear Aerodynamic Damping", AIAA Journal, Vol. 1, June 1963, pp. 1418-1419.

2. Tobak, M., Schiff, L.B. and Peterson, V.L., "Aerodynamics of Bodies of Revolution in Coning Motion", AIAA Journal, Vol. 7, January 1969, pp. 95-99.

3. Jaffe, P. "Nonplanar Tests Using the Wind-Tunnel Free-Flight Technique", J. Spacecraft and Rockets, Vol. 10, July 1973, pp. 435-442.

4. Tobak, M. and Schiff, L.B., "On the Formulation of the Aerodynamic Characteristics in Aircraft Dynamics", NASA TR R-456, January 1976.

5. Ericsson, L.E. and Beyers, M.E., "Nonplanar Motion Effects", AIAA-88-0215, January 1988.

6. Ericsson, L.E., "Wing Rock Generated by Forebody Vortices", AIAA-87-0268, January 1987.

7. Ericsson, L.E., "Flat Spin of Axisymmetrical Bodies in the Critical Reynolds Number Region", J. Spacecraft, Vol. 24, Nov.-Dec. 1987, pp. 532-538.

8. Beyers, M.E., "Aerodynamic Simulation of Multi-Degree-of-Freedom Aircraft Motion", ICIASF '81 Proceedings, September 1981.

9. Beyers, M.E., "Characteristic Motions for Simulations of Post-Stall Manoeuvres and Flight Instabilities", AeSSA/SAIAeE Journal, Vol. 5, No. 1, 1984, pp. 20-34.

10. Elzebda, J.M., Mook, D.T. and Nayfeh, A.H., "The Influence of an Additional Degree of Freedom on Subsonic Wing Rock of Slender Delta Wings", AIAA-87-0496, January 1987.

11. Scher, S.H., "An Analytical Investigation of Airplane Spin Recovery Motion by Use of Rotary Balance Aerodynamic Data", NACA TN 3188, 1954.

12. Malcolm, G.N. and Clarkson, M.H., "Wind-Tunnel Testing with a Rotary-Balance Apparatus to Simulate Aircraft Spin Motions", AIAA 9th Aerodynamic Testing Conference, Vol. II, June 1976, pp. 143-156.

13. Ericsson, L.E. and Reding, J.P., "Dynamic Support Interference in High Alpha Testing", J. Aircraft, Vol. 23, December 1986, pp. 889-896.

14. Beyers, M.E., "Wind-Tunnel Wall Interference in Rotary Balance Testing", NRC NAE-LTR-UA-90, Ottawa, November 1987.

15. Orlik-Rückemann, K.J., "Dynamic Stability Testing of Aircraft - Needs versus Capabilities", Progress in Aerospace Sciences, Vol. 16, No. 4, 1975, pp. 431-447.

16. Bihrle, W., Jr. and Barnhart, B., "Spin Prediction Techniques", J. Aircraft, Vol. 20, February 1983, pp. 97-101.

17. Beyers, M.E., "A New Concept for Aircraft Dynamic Stability Testing", J. Aircraft, Vol. 20, January 1983, pp. 5-14.

18. Huang, X.Z., "Rotary Balance with Gas Bearing Support", Rep. 1983.8, Beijing Institute of Aerodynamics (in Chinese), 1983.

19. Mandl, P. and Pounder, J.R., "Wind Tunnel Interference on Rolling Moment of a Rotating Wing", NRC AR-10, Ottawa, 1951.

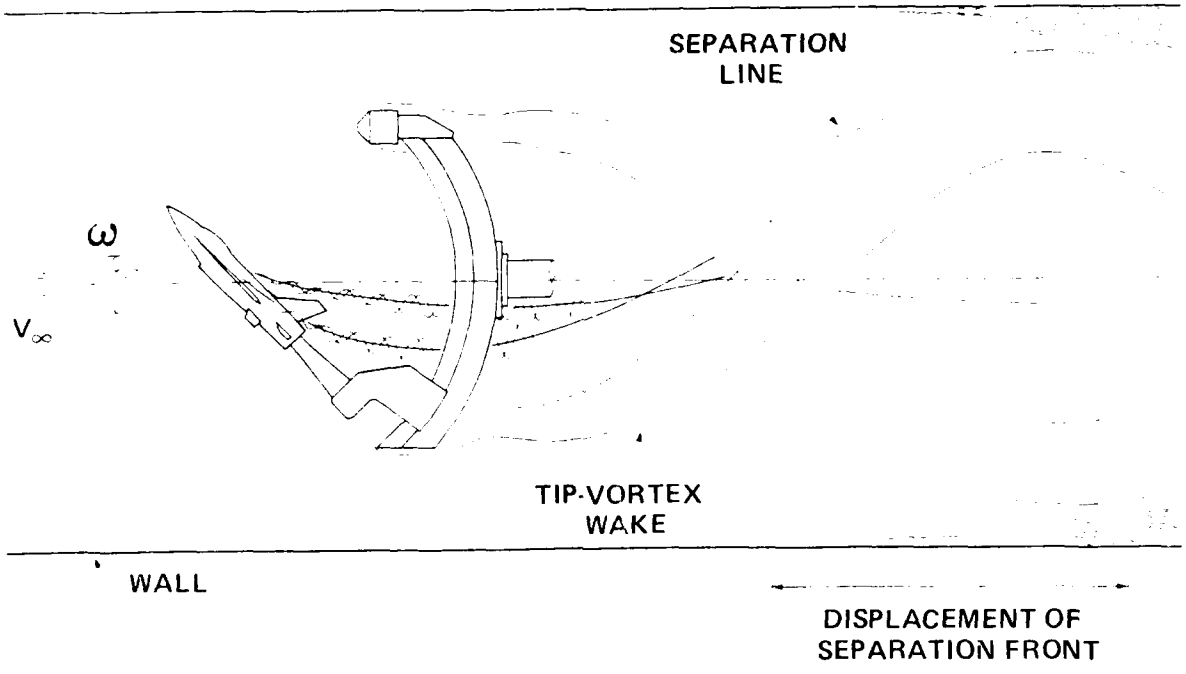

FIG. 1: AERODYNAMIC INTERFERENCE IN ROTARY TESTING

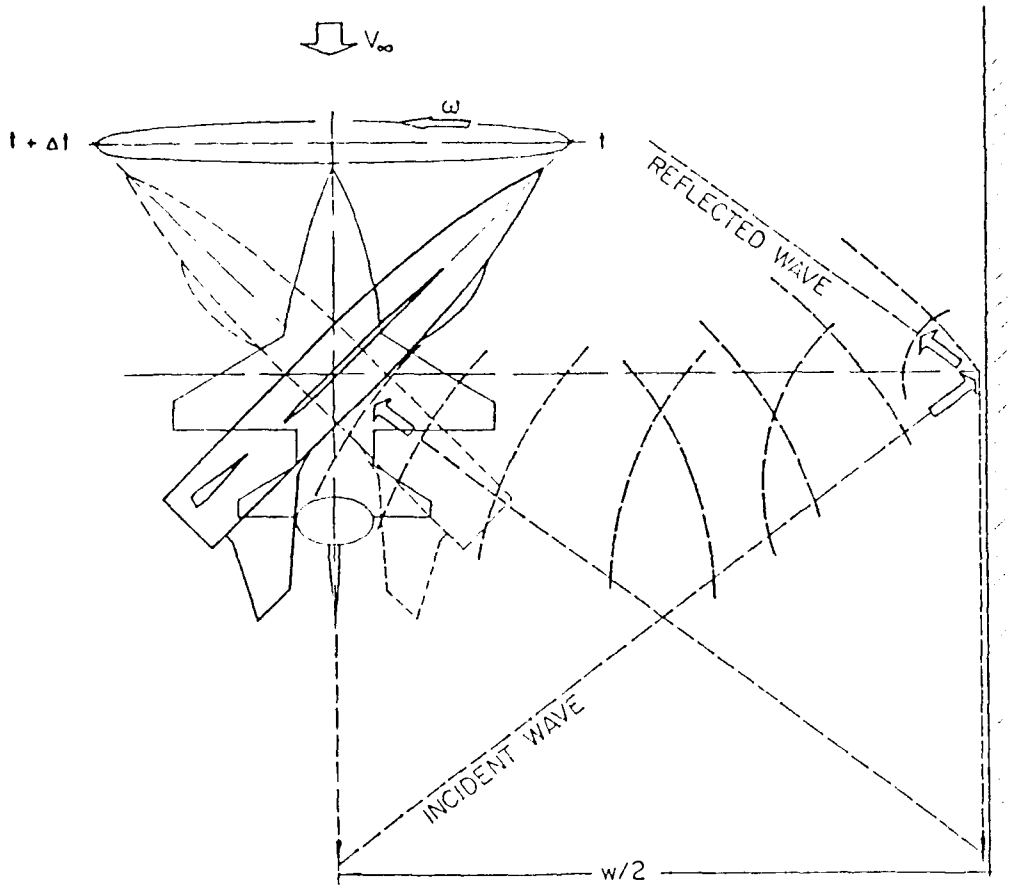

FIG. 2: TRANSVERSE ACOUSTIC INTERFERENCE ON CONING MODEL

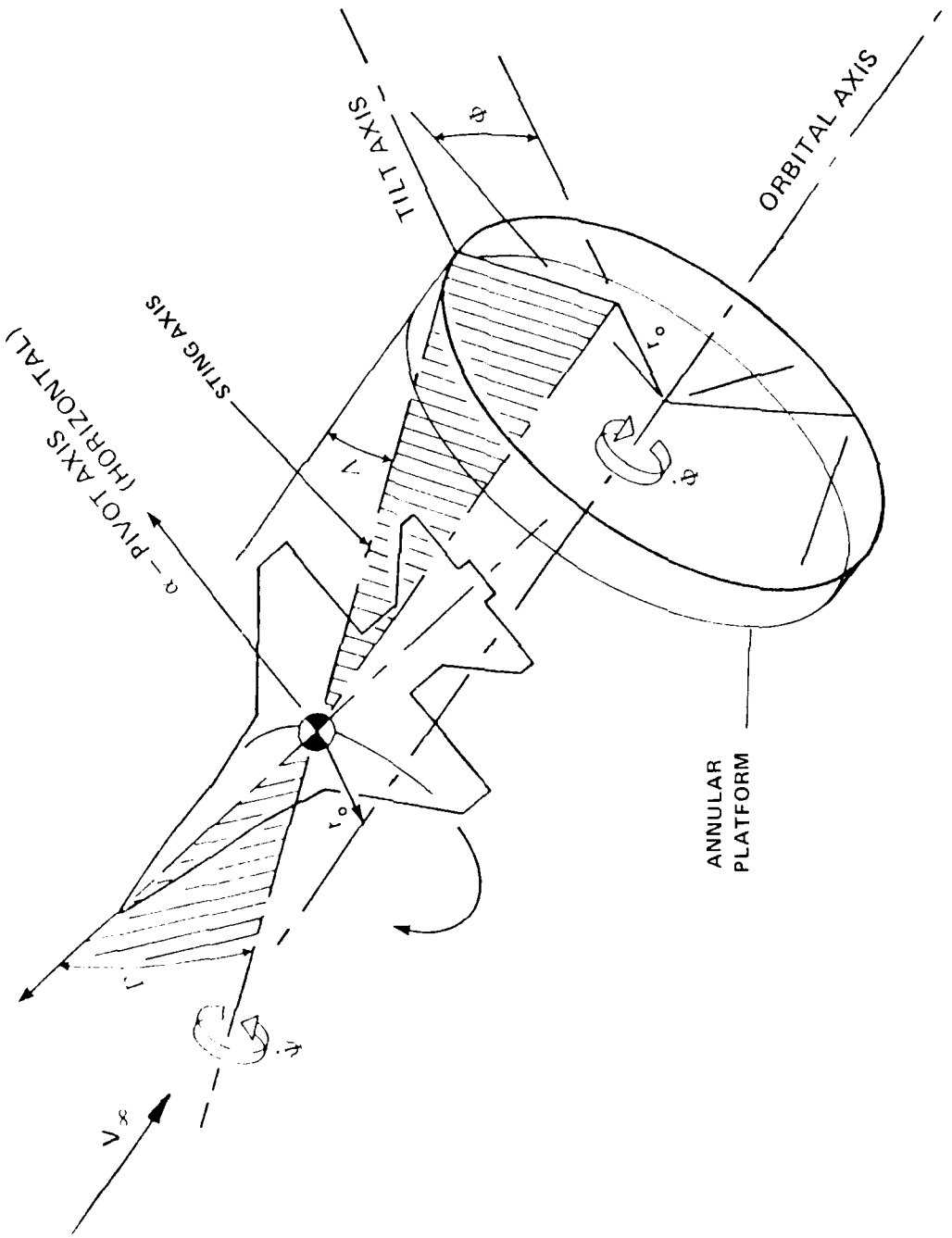

FIG. 3: ORBITAL MOTION GEOMETRY (HORIZONTAL AXIS)[17]

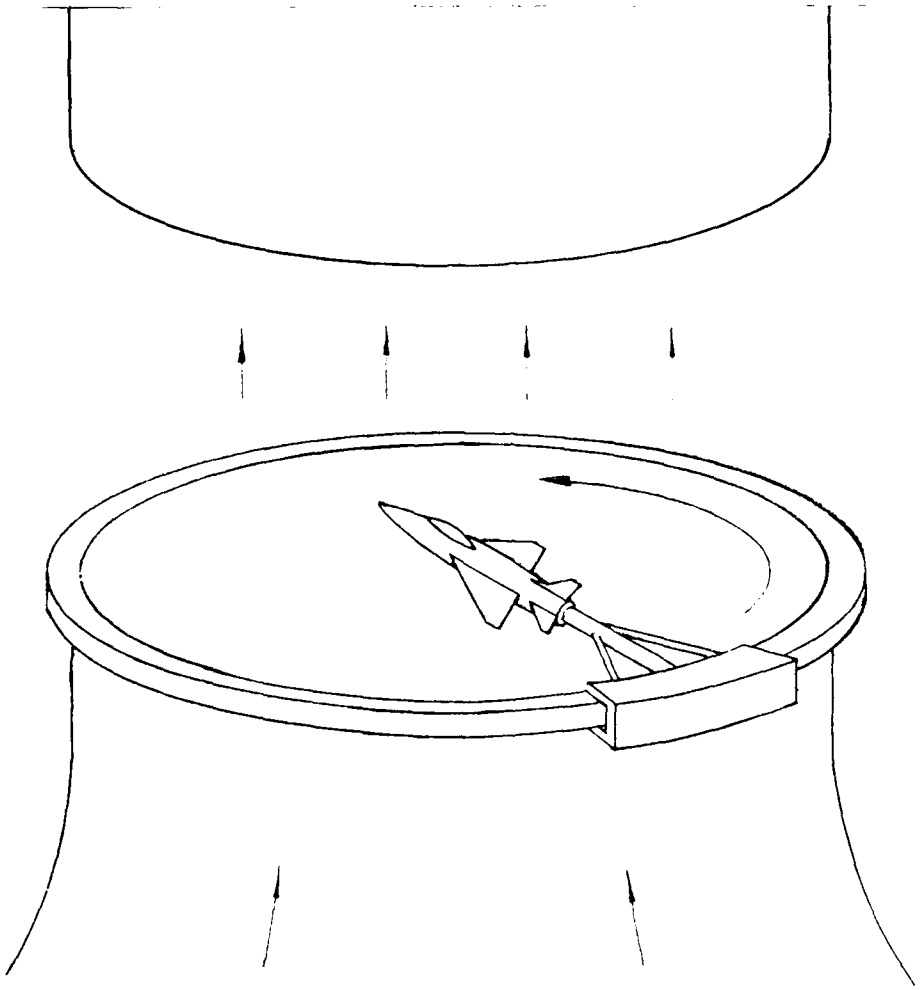

FIG. 4: ORBITAL-PLATFORM CONCEPT FOR VERTICAL TUNNEL

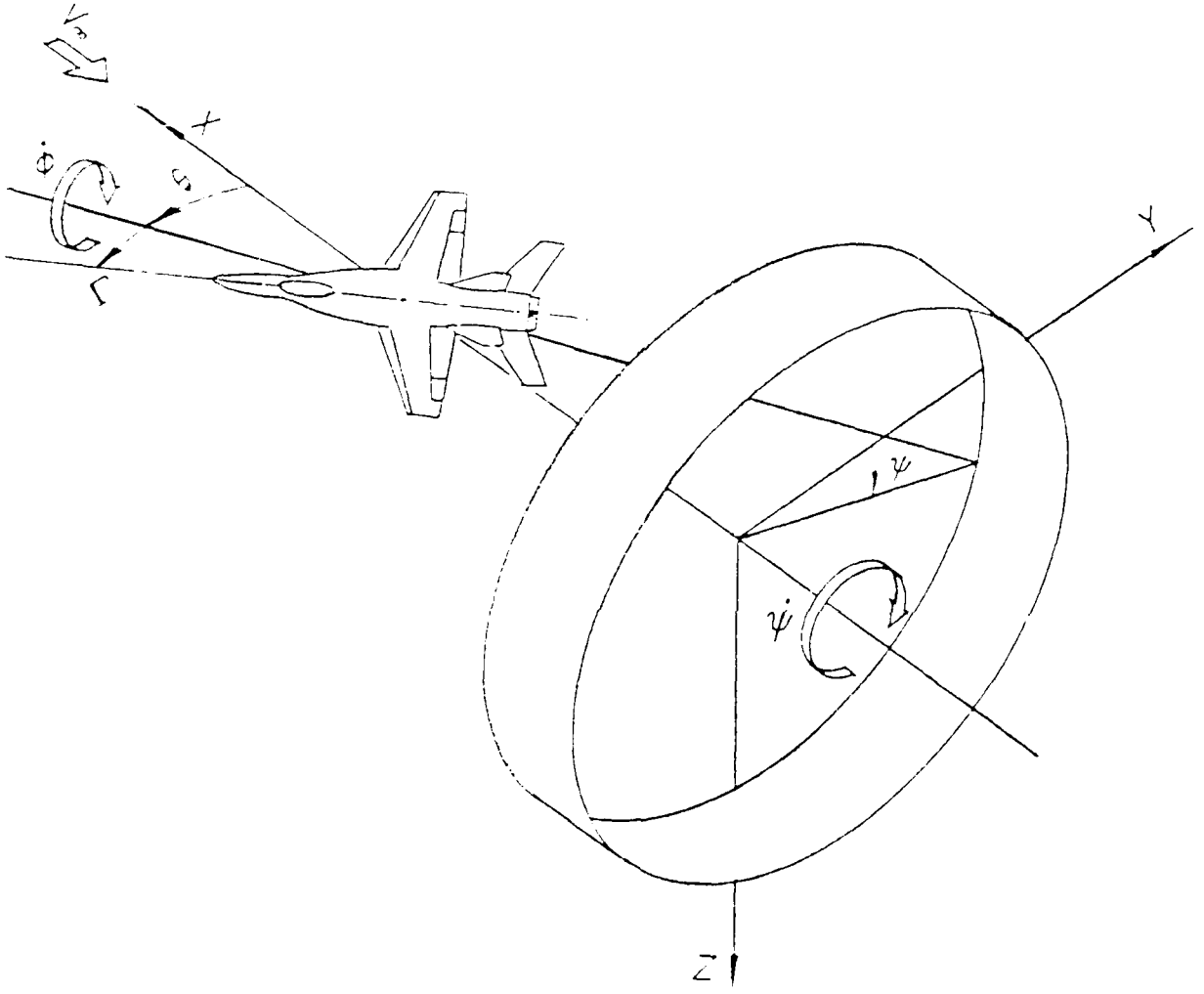

FIG. 5: EPICYCLIC MOTION GEOMETRY

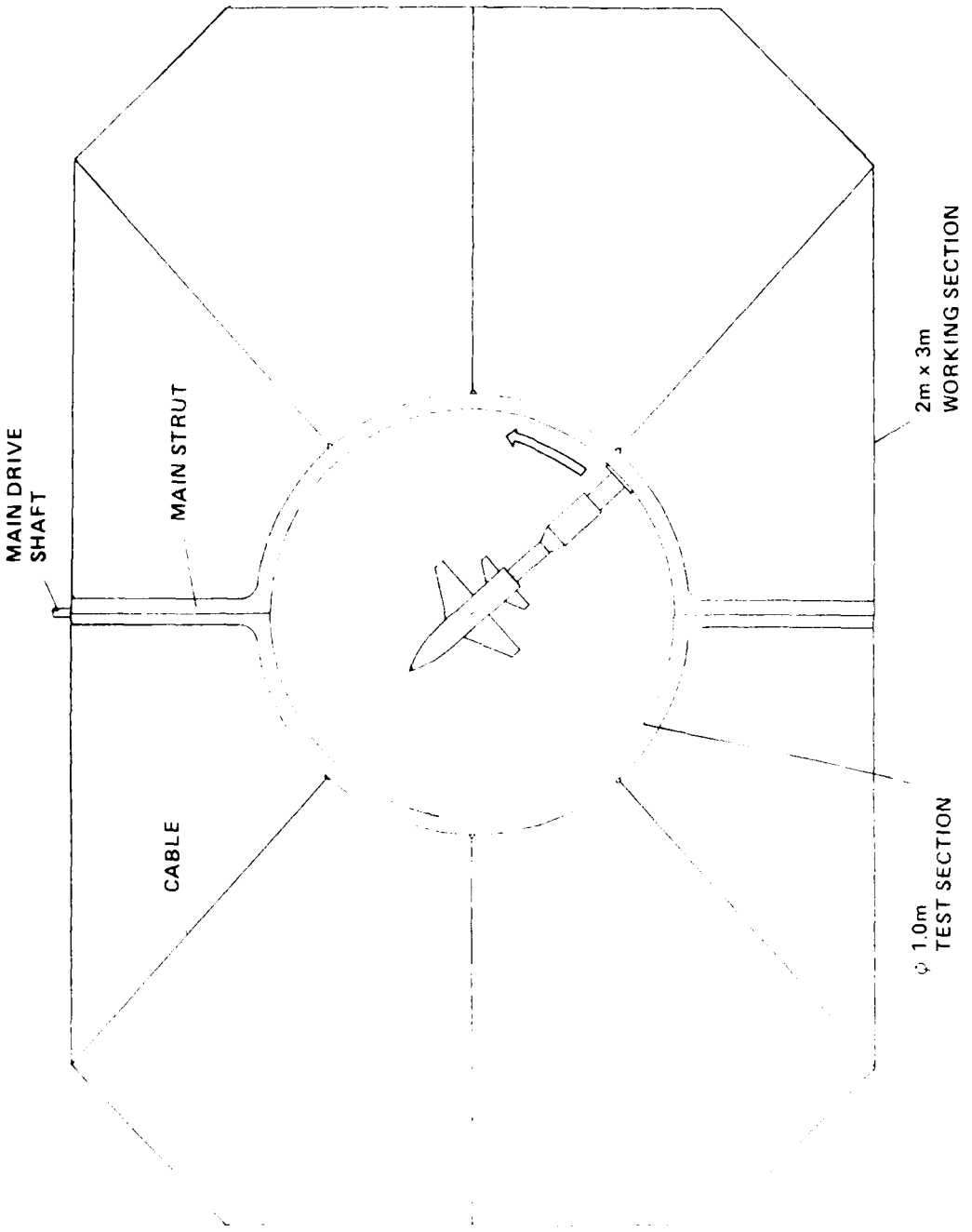

FIG. 6: LAYOUT IN 2m x 3m LOW SPEED WIND TUNNEL

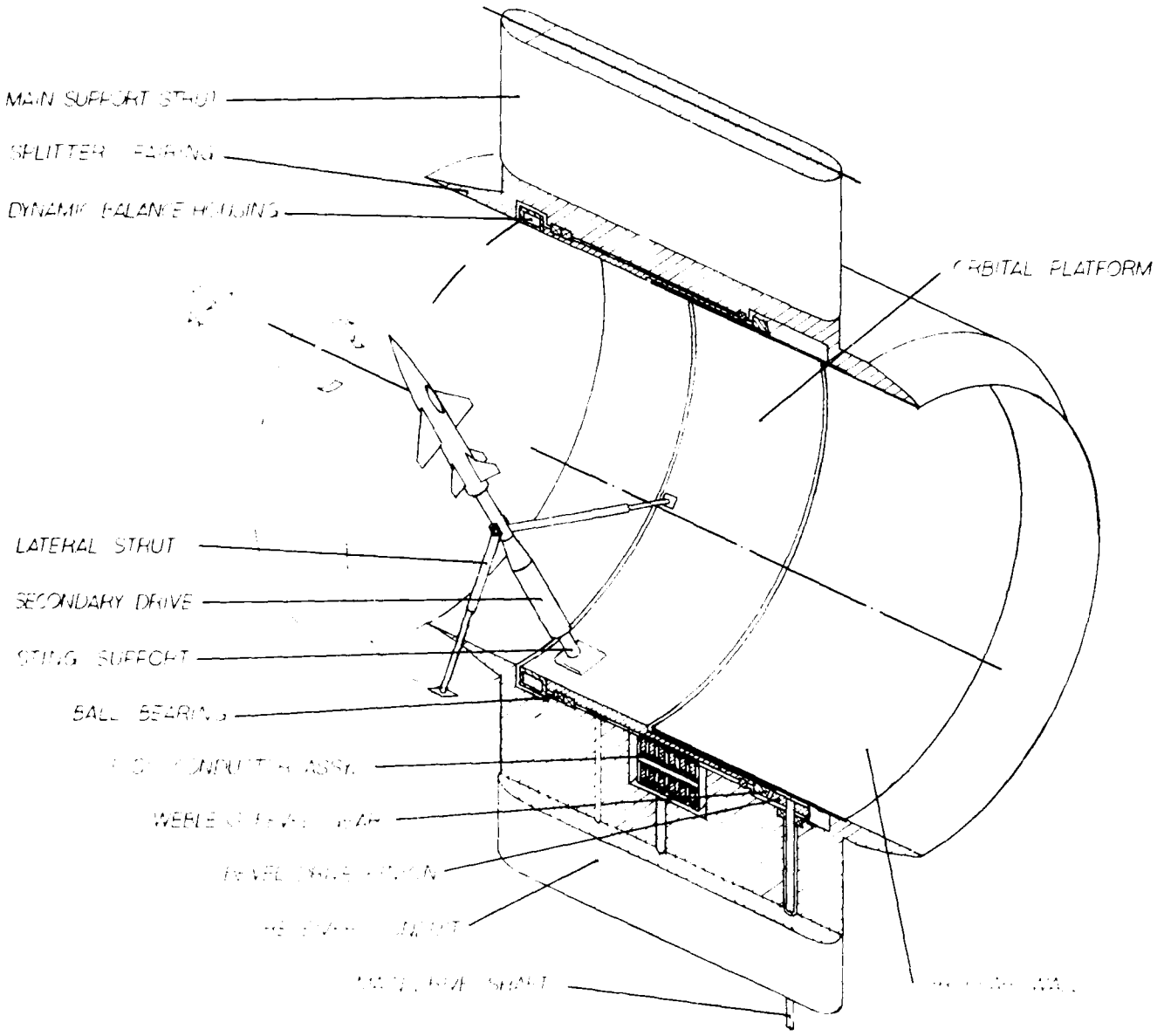

FIG. 7: LAYOUT OF OPLEC APPARATUS

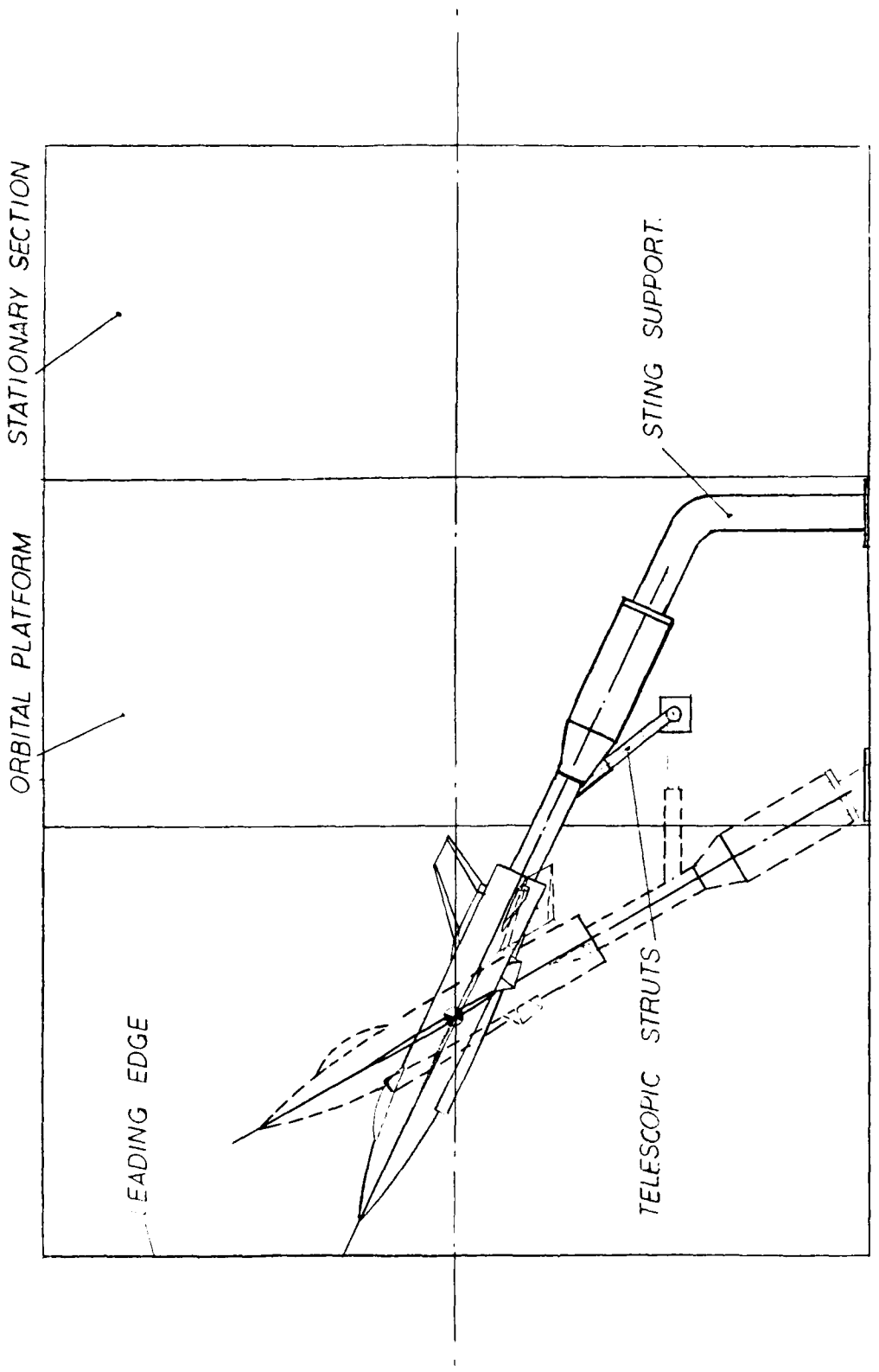

FIG. 8: PITCH ANGLE ADJUSTMENT

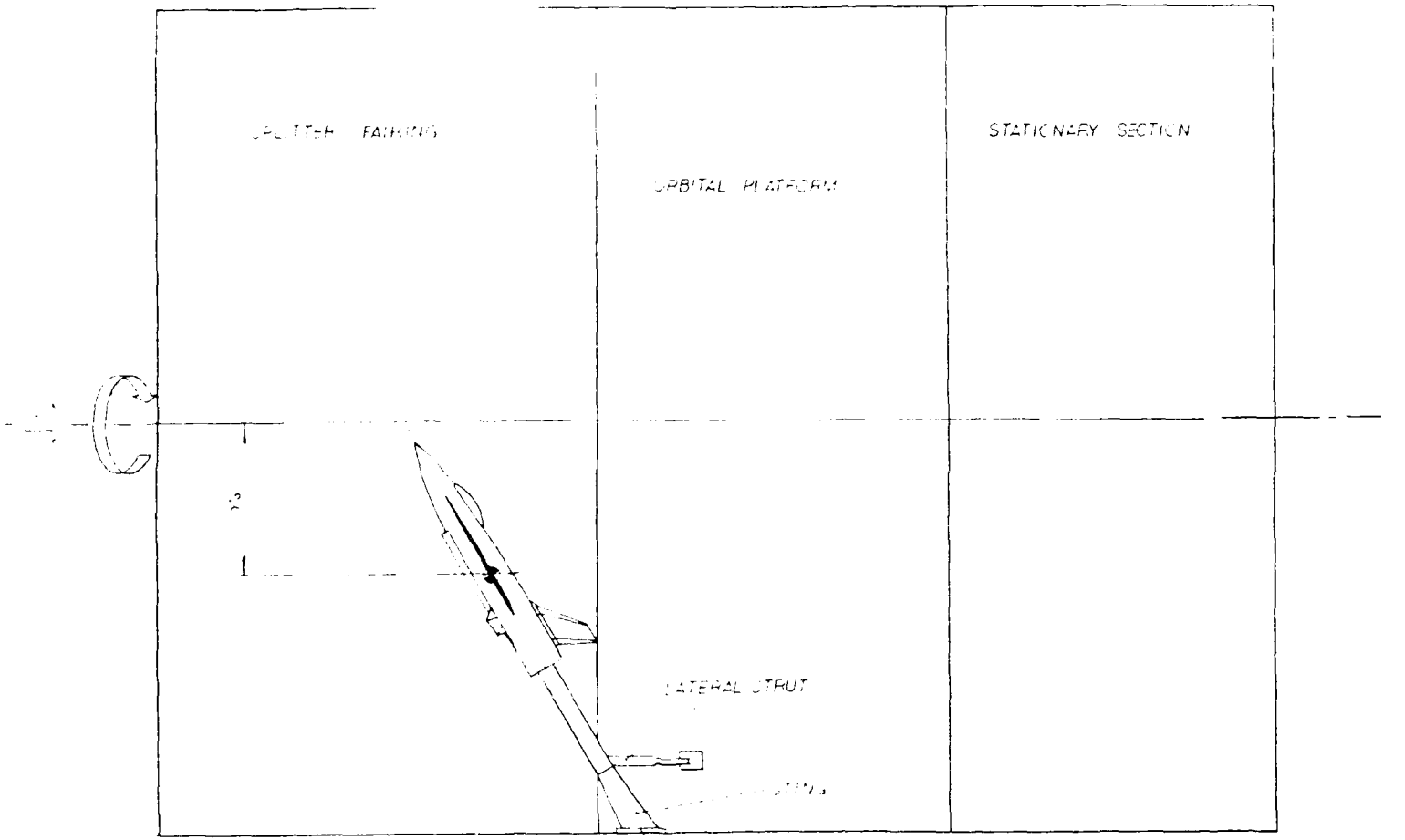

FIG. 9: SIMULATION OF STEADY SPIN ($r_o \neq 0$)

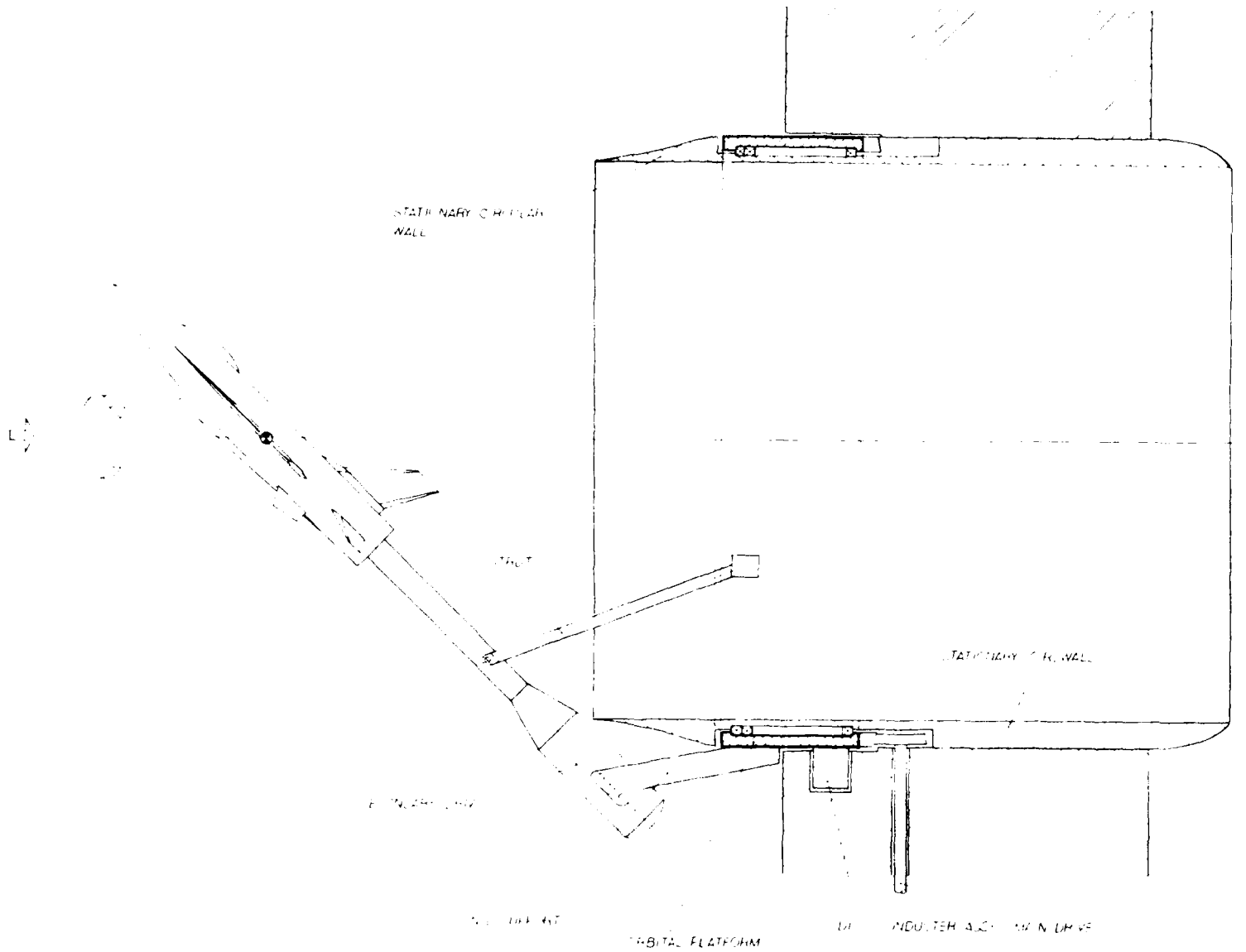

FIG. 10: EXTERNAL ORBITAL-PLATFORM CONCEPT

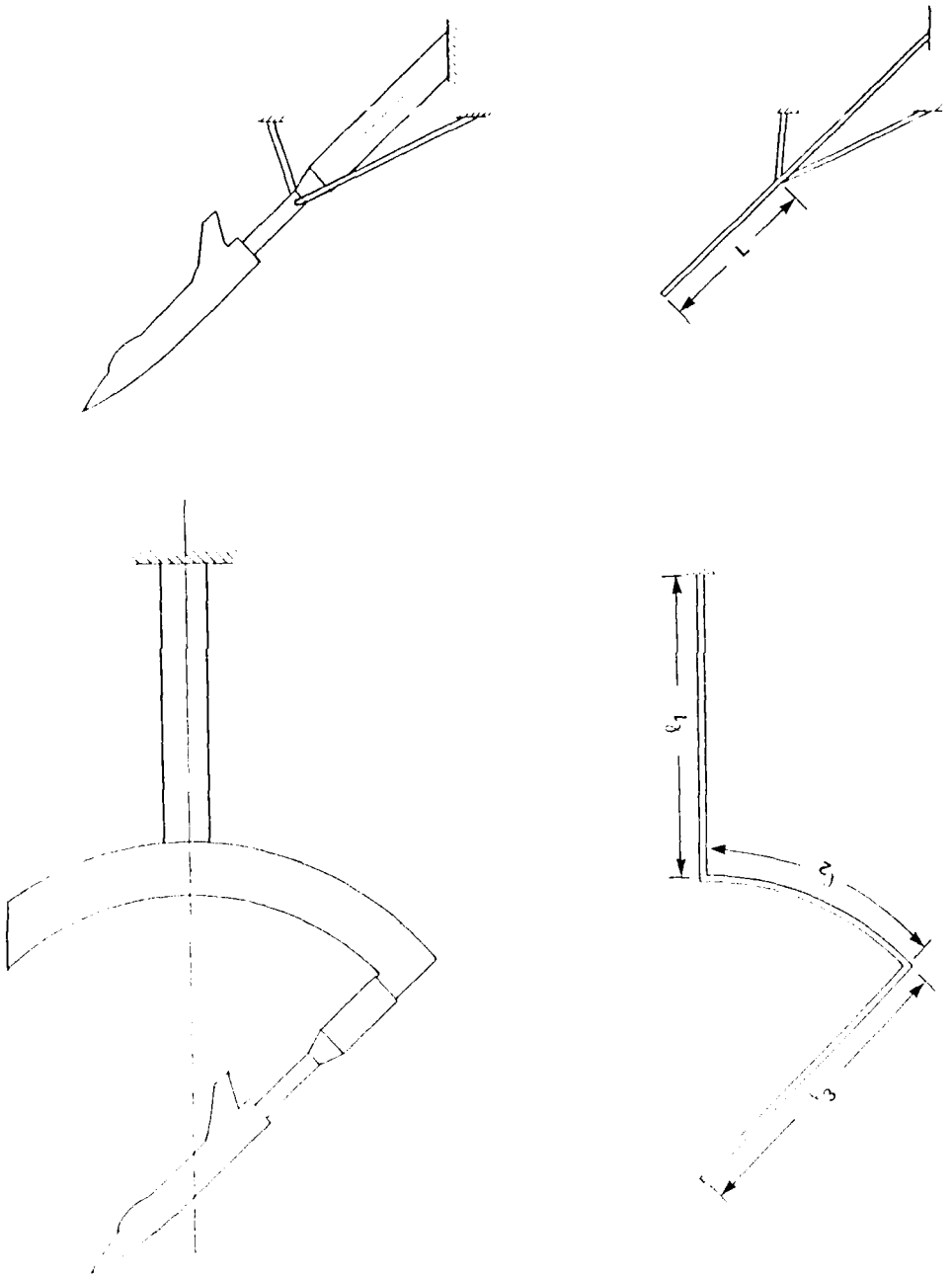

FIG. 11: STRUCTURAL COMPARISON

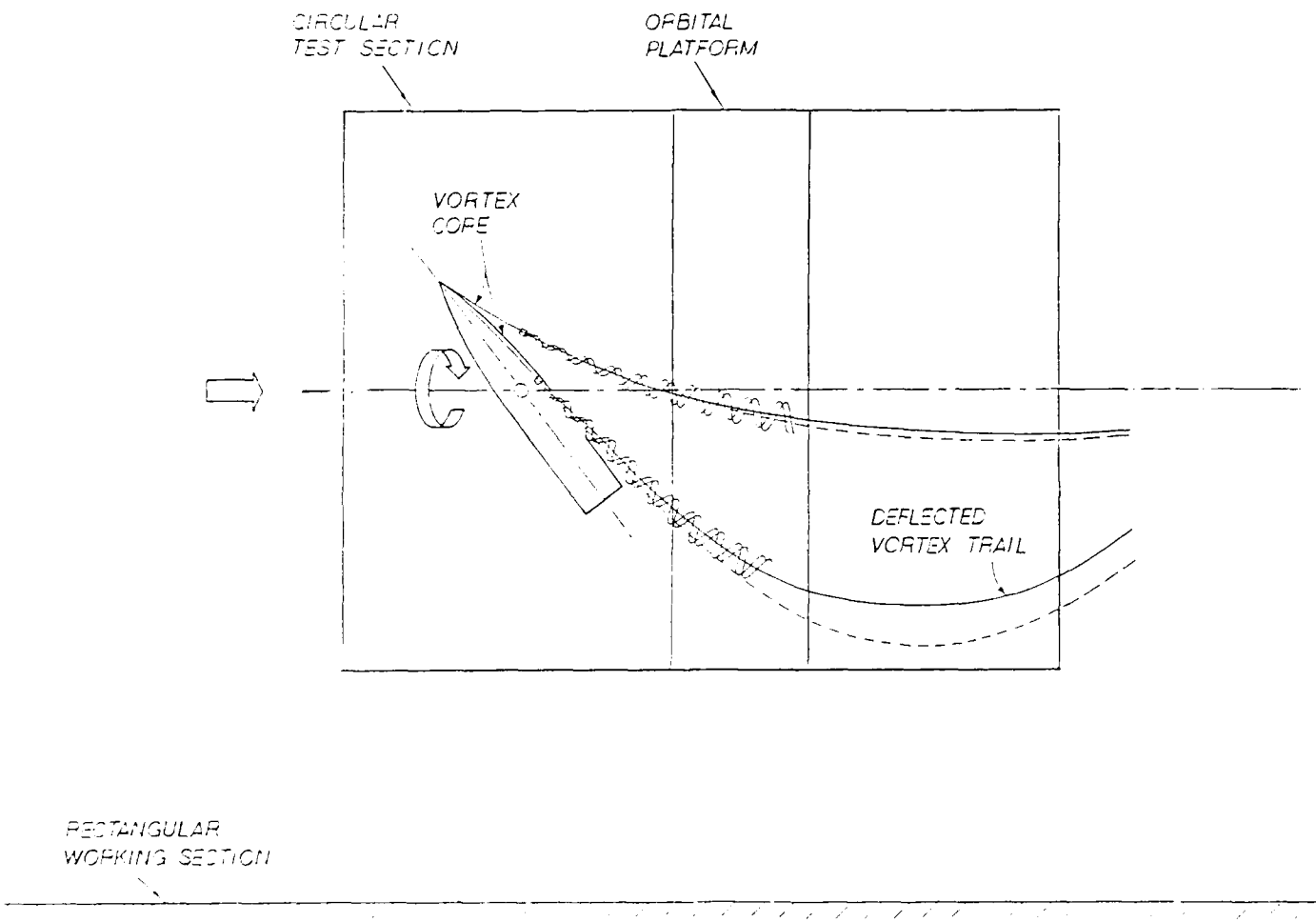

FIG. 12: VORTEX-WAKE/WALL INTERACTION

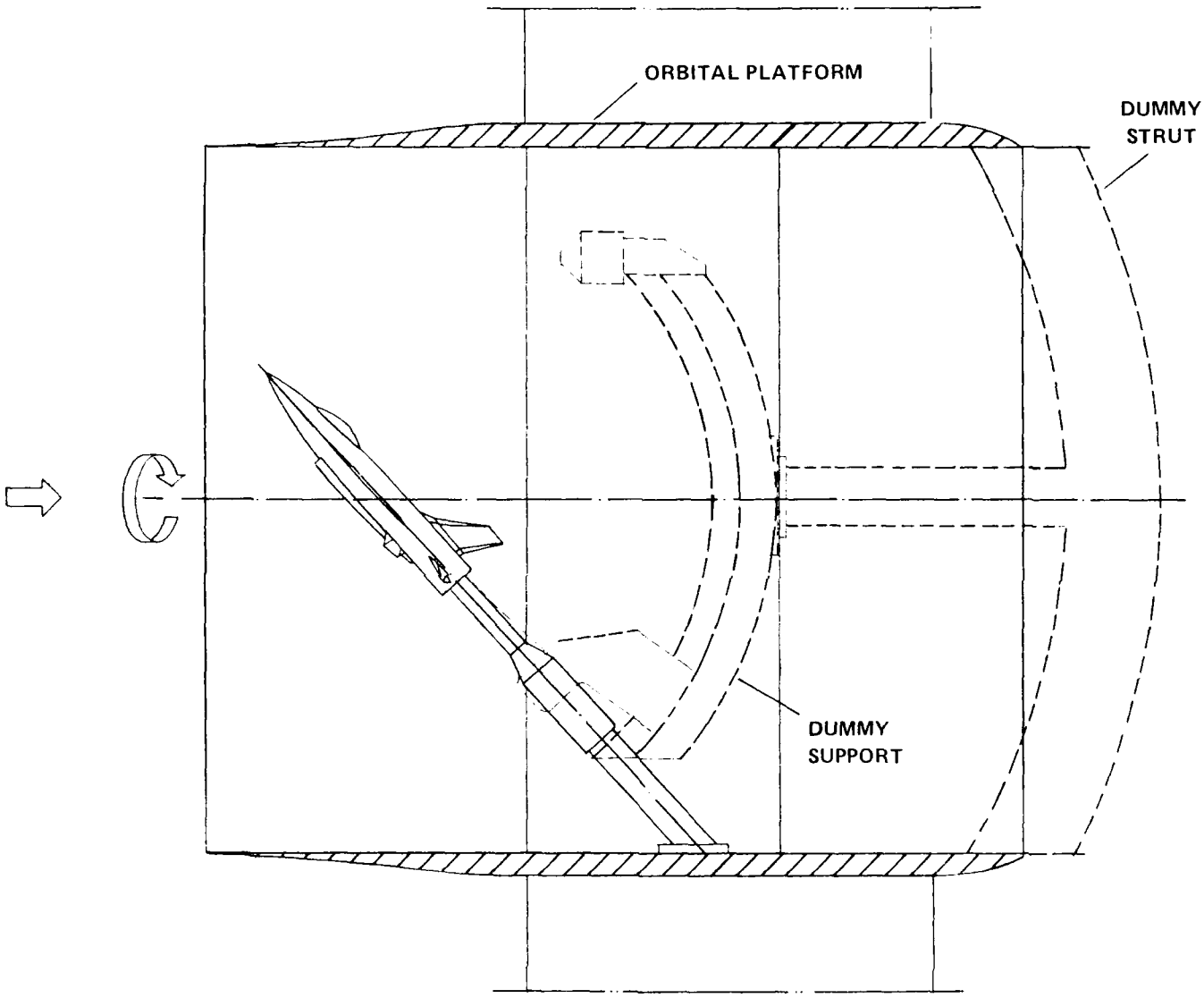

FIG. 13: INVESTIGATION OF SUPPORT INTERFERENCE

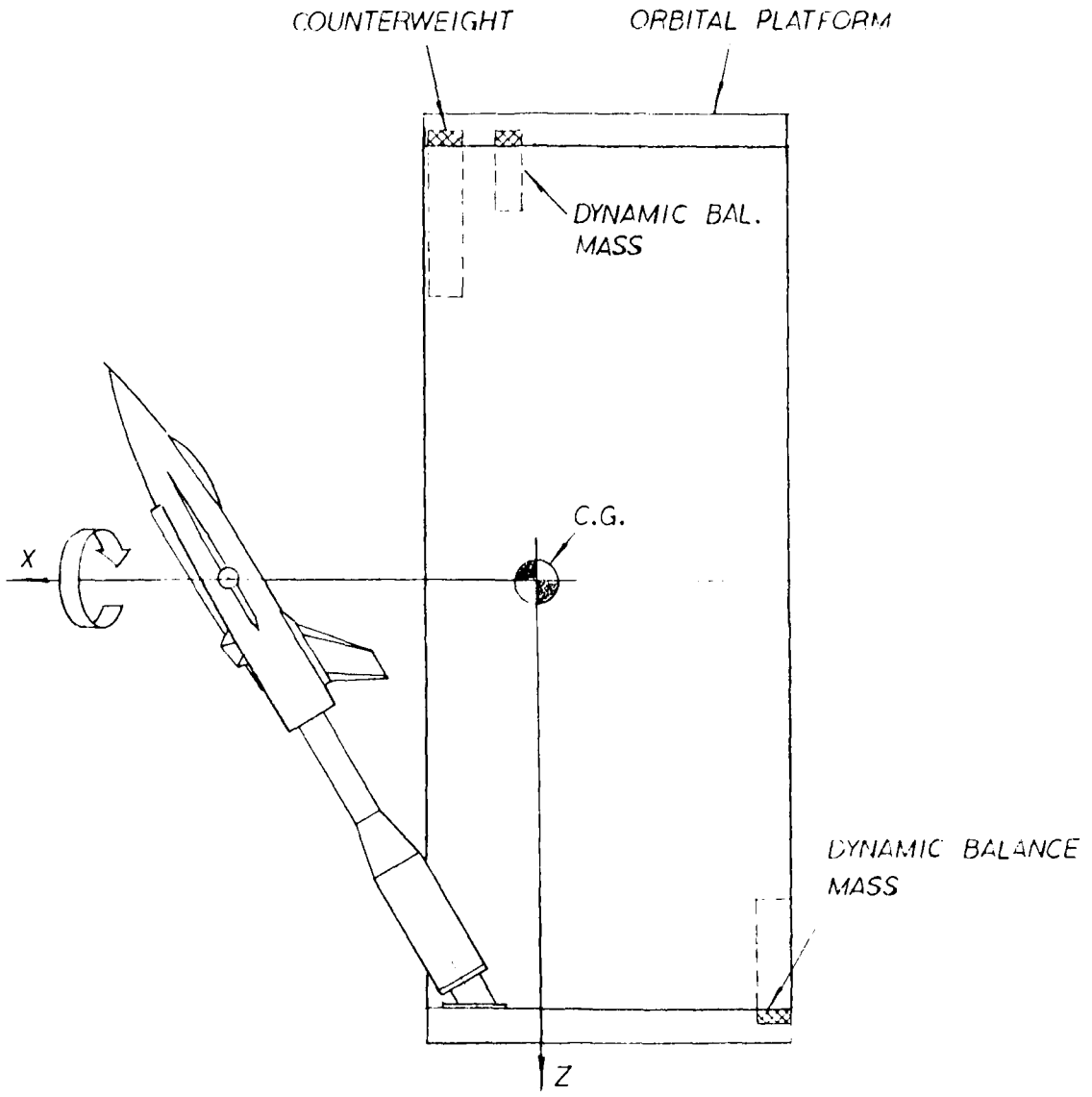

FIG. 14: DYNAMIC BALANCING SCHEME

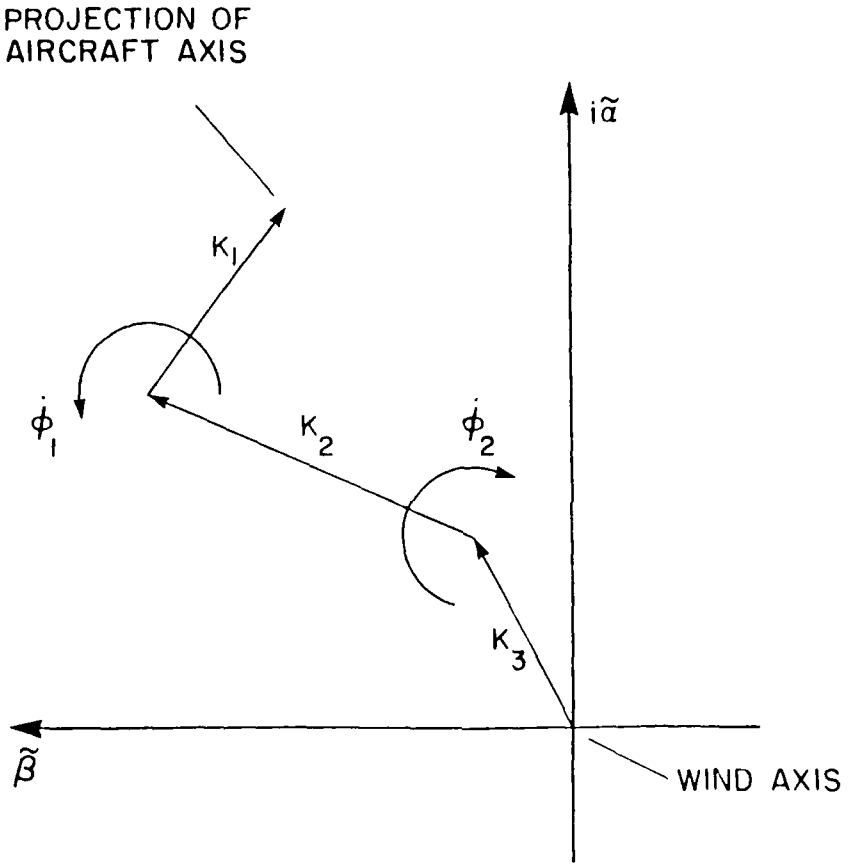

FIG. 15: EPICYCLIC MOTION

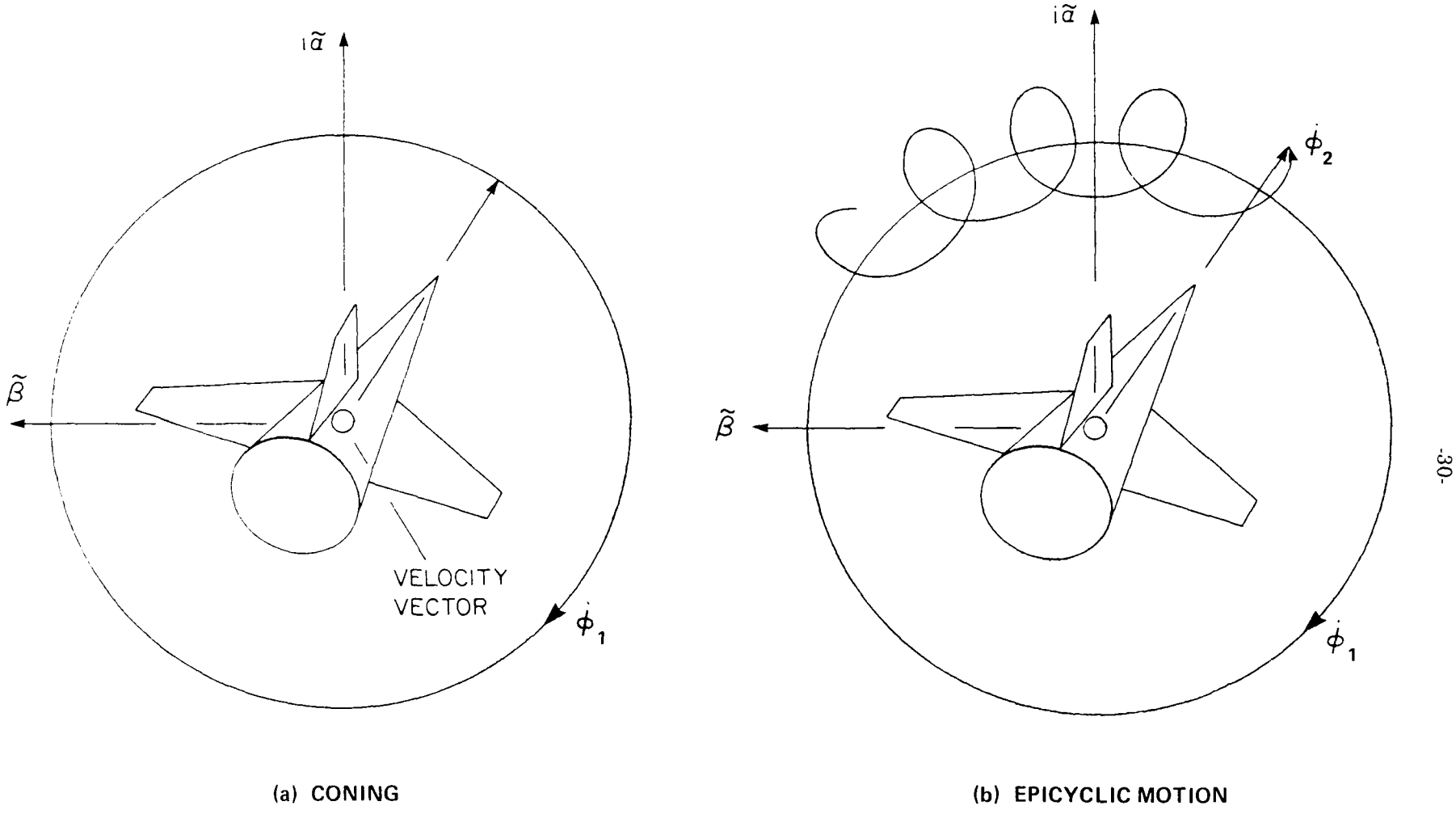

(a) CONING

(b) EPICYCLIC MOTION

FIG. 16: NONPLANAR CHARACTERISTIC MOTIONS

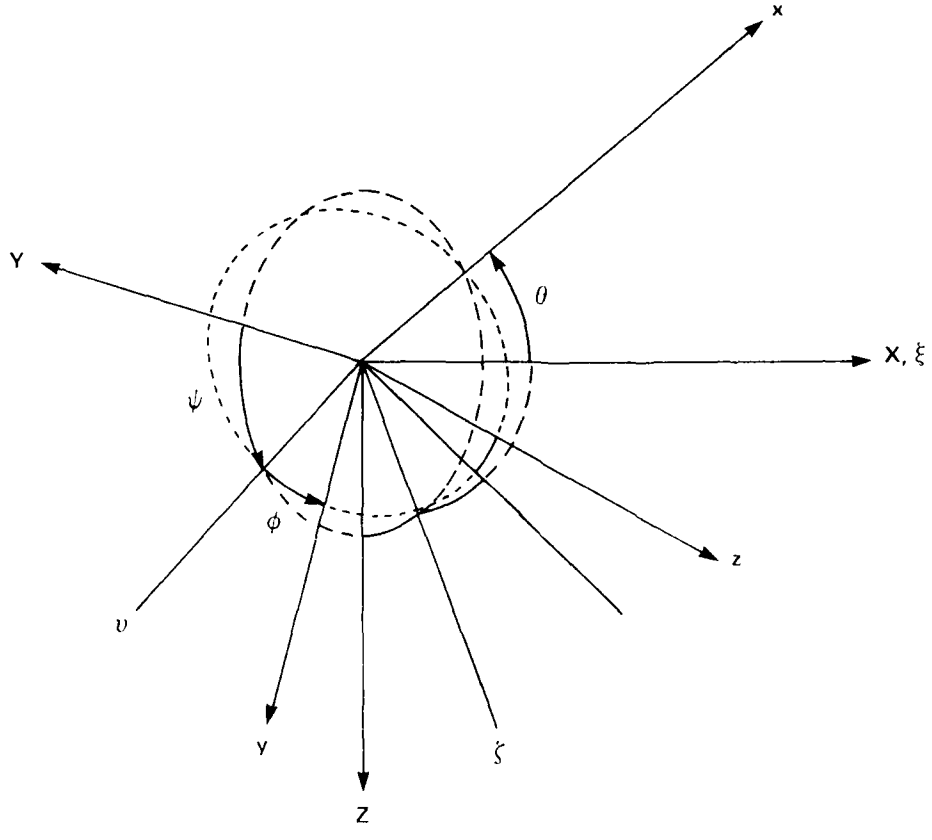

FIG. 17: REFERENCE SYSTEMS

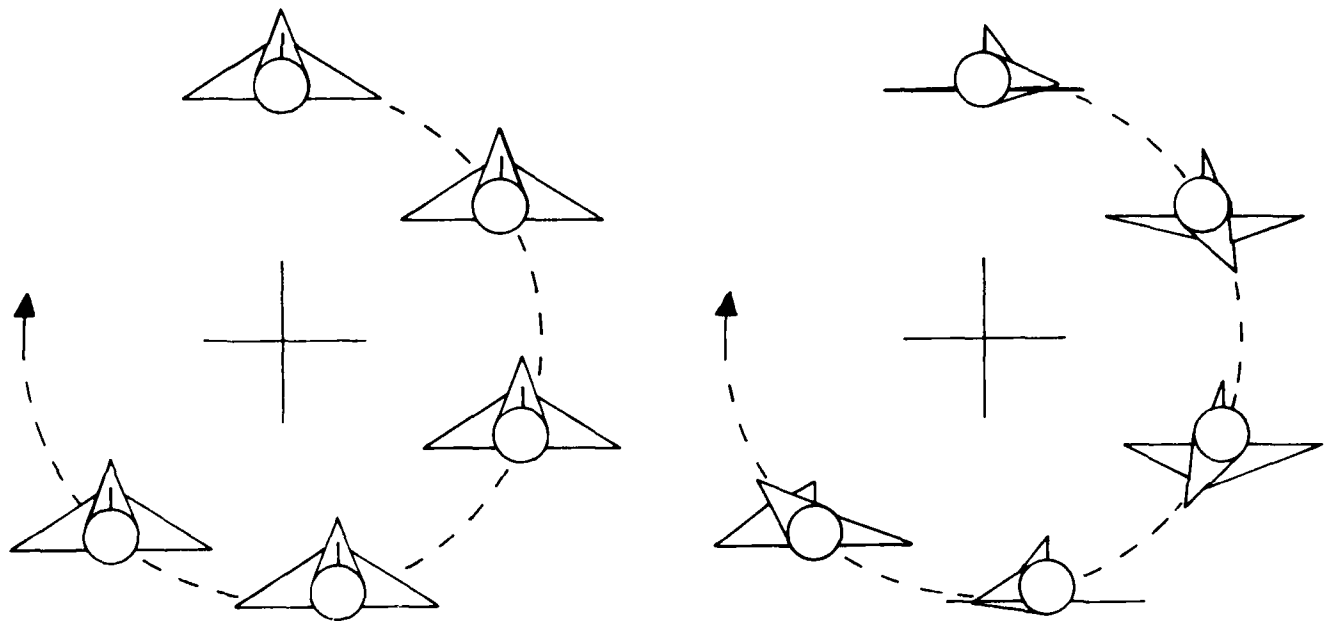

FIG. 18: ORBITAL FIXED-PLANE MOTION

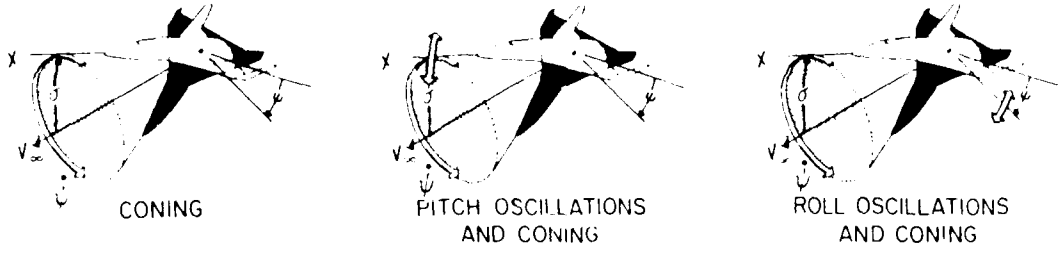

FIG. 19: CHARACTERISTIC MOTIONS IN AERODYNAMIC AXES SYSTEM[4]

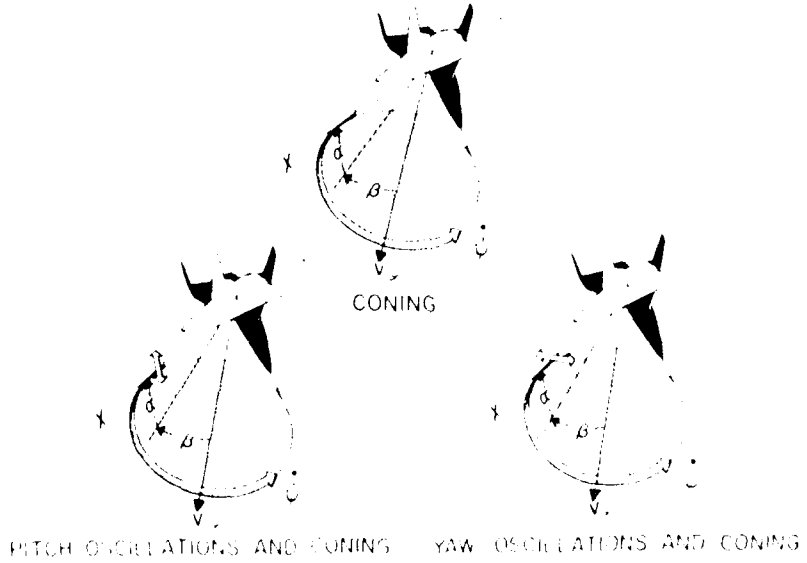

FIG. 20: CHARACTERISTIC MOTIONS IN BODY AXES SYSTEM[4]

REPORT DOCUMENTATION PAGE / PAGE DE DOCUMENTATION DE RAPPORT

REPORT/RAPPORT	REPORT/RAPPORT
NAE-AN-52 (1a)	NRC No. 29133 (1b)
REPORT SECURITY CLASSIFICATION / CLASSIFICATION DE SÉCURITÉ DE RAPPORT	DISTRIBUTION (LIMITATIONS)
Unclassified (2)	Unlimited (3)

TITLE/SUBTITLE/TITRE/SOUS-TITRE

The Orbital-Platform Concept for Nonplanar Dynamic Testing (4)

AUTHOR(S)/AUTEUR(S)

M.E. Beyers and X.Z. Huang (5)

SERIES/SÉRIE

Aeronautical Note (6)

CORPORATE AUTHOR/PERFORMING AGENCY/AUTEUR D'ENTREPRISE/AGENCE D'EXÉCUTION

National Research Council Canada
National Aeronautical Establishment — Unsteady Aerodynamics Laboratory (7)

SPONSORING AGENCY/AGENCE DE SUBVENTION

(8)

DATE	FILE/DOSSIER	LAB. ORDER / COMMANDE DU LAB.	PAGES	FIGS/DIAGRAMMES
88-05 (9)	(10)	(11)	40 (12a)	20 (12b)

NOTES

(13)

DESCRIPTORS (KEY WORDS)/MOTS-CLÉS

1. Dynamic tests — Nonplanar
2. Orbital space stations — Aerodynamic testing

(14)

SUMMARY/SOMMAIRE

A new concept is introduced for large-amplitude nonplanar testing at high incidence. The dynamic test apparatus is characterized by an annular, orbital platform on which the model support and secondary drive mechanisms are mounted. The device can be used as a rotary apparatus, while arbitrary epicyclic motions (including fixed-plane, orbital modes) and oscillatory motions superimposed on the coning mode may be generated. The system is inherently very rigid and vibration levels can be kept very low. Aerodynamic interference is also very low as there is no need for bulky support hardware and the test section is circular. Accordingly, the system may be used to assess levels of support interference in conventional rotary tests.

(15)